

Transfer matrix method for optics in graphene layers

Tianrong Zhan, Xi Shi, Yunyun Dai, Xiaohan Liu and Jian Zi*

*Department of Physics, Key Laboratory of Micro and Nano Photonic Structures (MOE),
and State Key Laboratory of Surface Physics, Fudan University, Shanghai 200433, P. R. China*

A transfer matrix method is developed for optical calculations of non-interacting graphene layers. Within the framework of this method, optical properties such as reflection, transmission and absorption for single-, double- and multi-layer graphene are studied. We also apply the method to structures consisting of periodically arranged graphene layers, revealing well-defined photonic band structures and even photonic bandgaps. Finally, we discuss graphene plasmons and introduce a simple way to tune the plasmon dispersion.

PACS numbers: 78.67.Wj, 78.20.Bh, 68.65.Pq, 78.67.Pt, 73.20.Mf

I. INTRODUCTION

Graphene is a flat monolayer of graphite with carbon atoms closely packed in a two-dimensional honeycomb lattice. A hallmark of graphene is the existence of Dirac cones in the electronic band structure, resulting in extraordinary structural and electronic properties with great potential for nanoelectronics [1–3].

In addition to outstanding electrical, mechanical and chemical properties, graphene has interesting optical response. One of the striking optical properties of graphene is that its reflectance, transmittance and absorbance are determined by the fine structure constant [4, 5]. Despite being only one-atomic-layer thick with negligible reflection, a single free-standing graphene shows significant absorbance, universally about 2.2% in a spectral range from near-infrared to visible [4, 6, 7]. In the infrared regime, graphene absorption can be altered by applying gate voltages [8, 9]. For few-layer graphene, the optical absorption is proportional to the number of layers [10], leading to a visual image contrast which can be used practically to identify the number of graphene layers on a substrate. The highly transparent and outstanding electrical properties of graphene make it attractive as transparent electrodes [11, 12]. The broadband absorption implies that graphene has the potential as an active medium used in broadband photodetectors [13, 14], ultra-fast lasers [15] and optical modulations [16].

In doped or gated graphene, collective excitations—plasmons exist with interesting optical features such as deep subwavelength and high confinement of optical fields [17–23], similar to surface plasmons in metal surfaces [24–26]. As a result, graphene may serve as a one-atom-thick platform for infrared and terahertz metamaterials [27, 28]. A number of photonic devices such as waveguides, splitters and combiners and superlenses could be envisioned [28, 29]. Numerical simulations suggest that periodically patterned arrays of doped graphene nanodisks may completely absorb infrared light at certain resonant wavelengths [30], which was soon confirmed ex-

perimentally [31]. These interesting optical properties of graphene may also offer potential applications in photonics [32].

In this paper, we develop a transfer matrix method for studying optical properties in non-interacting graphene layers. This paper is organized as follows. In section II, we introduce the transfer matrix method for studying the propagation of light through graphene layers, together with the optical conductivity of graphene used in our calculations. In Secs. III to V, we apply the transfer matrix method to the study of optics in graphene layers. Specifically, in section III we discuss reflection, transmission and absorption in single-, double- and multi-layer graphene. In section IV, we discuss photonic band structures in periodical graphene layers. In section V, we discuss plasmons in graphene. Finally, we present our summary in section VI.

II. GENERAL FORMULATION

Transfer matrix method is a powerful tool in the analysis of light propagations through layered dielectric media [33, 34]. The central idea lies that electric or magnetic fields in one position can be related to those in other positions through a transfer matrix. Within the framework of the transfer matrix method, there are two kinds of matrices: one is the transmission matrix that connects the fields across an interface and the other is the propagation matrix that connects the fields propagating over a distance within a homogeneous medium.

A. Transmission matrix

We first consider the propagation of light across an interface formed by a graphene layer which separates two dielectrics of dielectric constants ϵ_1 and ϵ_2 , as shown schematically in figure 1(a). The graphene layer has an optical conductivity σ lying at $z = 0$. Light is assumed to be polarized in the y direction and propagate in the z direction. For structures considered, s and p polarizations can be decoupled. As a result, we can deal with s

* jzi@fudan.edu.cn

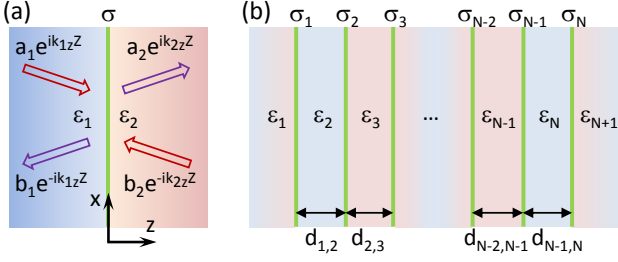


FIG. 1. (a) A single graphene layer surrounded by two dielectrics of dielectric constants ϵ_1 and ϵ_2 . The graphene layer is characterized by a conductivity σ . Red and purple arrows indicate incoming and outgoing light, respectively. (b) A stack of N graphene layers of conductivity σ_i ($i = 1, 2, \dots, N$) are separated by different dielectrics of dielectric constants ϵ_i ($i = 1, 2, \dots, N+1$). The spacing between two adjacent graphene layers is denoted by $d_{i,i+1}$ ($i = 1, 2, \dots, N-1$).

and p polarizations separately.

For p polarization, the magnetic field is polarized along the y direction and can be written as the form

$$H_{1y} = (a_1 e^{ik_{1z}z} + b_1 e^{-ik_{1z}z}) e^{ik_{1x}x}, \quad z < 0, \quad (1)$$

$$H_{2y} = (a_2 e^{ik_{2z}z} + b_2 e^{-ik_{2z}z}) e^{ik_{2x}x}, \quad z > 0. \quad (2)$$

Here, a_i and b_i ($i = 1, 2$) are the field coefficients, k_{ix} (k_{iz}) is the x (z) component of the wave-vector $k_i = \sqrt{\epsilon_i} \omega / c$, where ω is the angular frequency and c is the speed of light in vacuum. The first (second) term in the parenthesis on the right side represents propagating waves along the z ($-z$) direction. From the Snell's law, we will immediately have $k_{1x} = k_{2x}$.

The electric and magnetic fields at the interface can be related by the following boundary conditions [35]

$$\mathbf{n} \times (\mathbf{E}_2 - \mathbf{E}_1)|_{z=0} = 0, \quad (3)$$

$$\mathbf{n} \times (\mathbf{H}_2 - \mathbf{H}_1)|_{z=0} = \mathbf{J}, \quad (4)$$

where \mathbf{n} is the unit surface normal and \mathbf{J} is the surface current density of the graphene layer. Applying the above boundary conditions at $z = 0$, we will have

$$\frac{k_{1z}}{\epsilon_1} (a_1 - b_1) - \frac{k_{2z}}{\epsilon_2} (a_2 - b_2) = 0, \quad (5)$$

$$(a_1 + b_1) - (a_2 + b_2) = J_x. \quad (6)$$

Note that \mathbf{J} can be obtained from Ohm's law, namely

$$J_x = \sigma E_x|_{z=0} = \frac{\sigma k_{2z}}{\epsilon_0 \epsilon_2 \omega} (a_2 - b_2), \quad (7)$$

where ϵ_0 is the vacuum permittivity. Combining equations (5)–(7), the coefficients a_1 and b_1 can be related to a_2 and b_2 by a 2×2 transmission matrix $D_{1 \rightarrow 2}$

$$\begin{bmatrix} a_1 \\ b_1 \end{bmatrix} = D_{1 \rightarrow 2} \begin{bmatrix} a_2 \\ b_2 \end{bmatrix}, \quad (8)$$

where

$$D_{1 \rightarrow 2} = \frac{1}{2} \begin{bmatrix} 1 + \eta_p + \xi_p & 1 - \eta_p - \xi_p \\ 1 - \eta_p + \xi_p & 1 + \eta_p - \xi_p \end{bmatrix}, \quad (9)$$

with the parameters η_p and ξ_p given by

$$\eta_p = \frac{\epsilon_1 k_{2z}}{\epsilon_2 k_{1z}}, \quad \xi_p = \frac{\sigma k_{2z}}{\epsilon_0 \epsilon_2 \omega}. \quad (10)$$

For s polarization, the electric field is polarized along the y direction. Similarly, by applying the boundary conditions and Ohm's law, the transmission matrix for s polarization that relates the electric fields at the two sides of the interface can be obtained, as

$$D_{1 \rightarrow 2} = \frac{1}{2} \begin{bmatrix} 1 + \eta_s + \xi_s & 1 - \eta_s + \xi_s \\ 1 - \eta_s - \xi_s & 1 + \eta_s - \xi_s \end{bmatrix}, \quad (11)$$

with the parameters η_s and ξ_s given by

$$\eta_s = \frac{k_{2z}}{k_{1z}}, \quad \xi_s = \frac{\sigma \mu_0 \omega}{k_{1z}}, \quad (12)$$

where μ_0 is the vacuum permeability.

The transmission matrix for s and p polarizations across an interface has similar forms except for the sign of ξ in the off-diagonal elements. Introducing a polarization dependent parameter ς_m , the transmission matrix for both polarizations can have an identical form

$$D_{1 \rightarrow 2, m} = \frac{1}{2} \begin{bmatrix} 1 + \eta_m + \xi_m & 1 - \eta_m - \varsigma_m \xi_m \\ 1 - \eta_m + \varsigma_m \xi_m & 1 + \eta_m - \xi_m \end{bmatrix}, \quad (13)$$

where $m = (s, p)$ and $\varsigma_p = 1$ and $\varsigma_s = -1$.

B. Propagation matrix

We now consider the propagation of light in a homogeneous medium. It can be shown [33] that the electric or magnetic fields at $z + \Delta z$ can be related to those at the z position by a 2×2 propagation matrix

$$P(\Delta z) = \begin{bmatrix} e^{-ik_z \Delta z} & 0 \\ 0 & e^{ik_z \Delta z} \end{bmatrix}. \quad (14)$$

C. Transfer matrix for multi-layer graphene

For a stack of N graphene layers shown in figure 1(b), the transfer matrix can be obtained by transmission matrices across different interfaces and propagation matrices in different homogeneous dielectric media. Denote the field coefficients on the left side of the leftmost graphene layer by a_1 and b_1 and those on the right side of the rightmost graphene layer by a_{N+1} and b_{N+1} . The two sets of field coefficients are then related by a 2×2 transfer matrix \mathcal{M} , namely

$$\begin{bmatrix} a_1 \\ b_1 \end{bmatrix} = \mathcal{M} \begin{bmatrix} a_{N+1} \\ b_{N+1} \end{bmatrix}, \quad (15)$$

with

$$\mathcal{M} = D_{1 \rightarrow 2} P(d_{1,2}) D_{2 \rightarrow 3} P(d_{2,3}) \cdots P(d_{N-1,N}) D_{N \rightarrow N+1}. \quad (16)$$

D. Optical spectrum calculations

With the transfer matrix, we can easily calculate the optical spectra such as reflection, transmission and absorption for multi-layer graphene. Suppose that light is incident from left upon the multi-layer graphene with the reflection and transmission coefficients denoted respectively by r and t . It can be shown that these coefficients are given by the elements of \mathcal{M}

$$r = \frac{M_{21}}{M_{11}}, \quad (17)$$

$$t = \frac{1}{M_{11}}. \quad (18)$$

And reflectance and transmittance can be calculated for both s and p polarizations as

$$R_{s,p} = |r_{s,p}|^2, \quad (19)$$

$$T_{s,p} = \eta_{s,p} |t_{s,p}|^2, \quad (20)$$

where

$$\eta_s = k_{(N+1)z}/k_{1z}, \quad \eta_p = \varepsilon_1 k_{(N+1)z}/\varepsilon_{N+1} k_{1z}. \quad (21)$$

Absorbance can then be readily obtained from

$$A = 1 - R - T. \quad (22)$$

E. Optical conductivity of graphene

For illustration and simplicity, in the present work we only consider the situation where the chemical potential of graphene μ is much larger than the temperature. In this situation, within the random-phase approximation the optical conductivity of graphene $\sigma(\omega)$ is given by [17–19, 36–38]

$$\frac{\sigma(\Omega)}{\varepsilon_0 c} = 4\alpha \frac{i}{\Omega} + \pi\alpha \left[\vartheta(\Omega - 2) + \frac{i}{\pi} \ln \left| \frac{\Omega - 2}{\Omega + 2} \right| \right]. \quad (23)$$

Here, $\Omega \equiv \hbar\omega/\mu$ is the dimensionless frequency, $\alpha \equiv e^2/4\pi\varepsilon_0\hbar c$ ($\sim 1/137$) is the fine structure constant and $\vartheta(x)$ is the Heaviside step function. The first and second terms on the right side stem from the intraband and interband contributions, respectively.

III. REFLECTION, TRANSMISSION AND ABSORPTION

A. Single-layer graphene

For a single graphene layer surrounded by two dielectrics of dielectric constants ε_1 and ε_2 , suppose that light is incident from the dielectric medium of ε_1 . The transfer matrix is no other than the transmission matrix across the interface, given by equations (9) and (11)

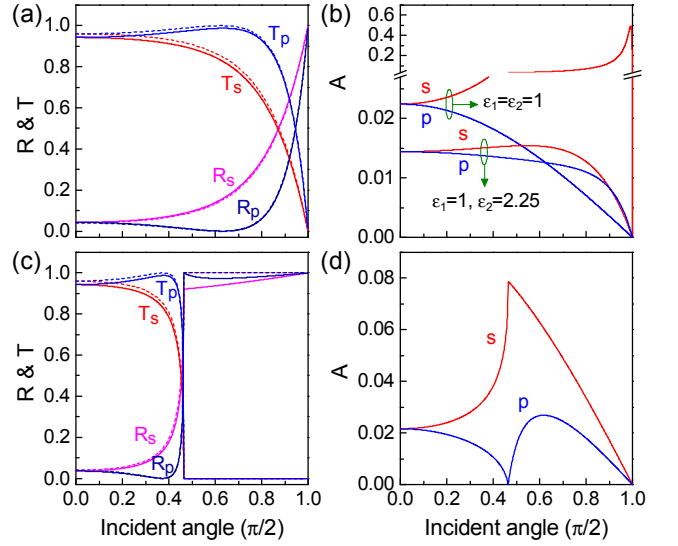


FIG. 2. Reflectance, transmittance and absorbance of single-layer graphene as a function of the incident angle for $\Omega > 2$. (a) Reflectance and transmittance for s and p polarizations with $\varepsilon_1 = 1$ and $\varepsilon_2 = 2.25$. Dashed lines represent those in the absence of the graphene layer. (b) Absorbance for (i) $\varepsilon_1 = \varepsilon_2 = 1$ and (ii) $\varepsilon_1 = 1$ and $\varepsilon_2 = 2.25$. (c) Same as (a) but for $\varepsilon_1 = 2.25$ and $\varepsilon_2 = 1$. The corresponding absorbance is given in (d).

for p and s polarizations, respectively. From equations (19) and (20), the reflectance and transmittance can be obtained as

$$R_s = \left| \frac{\sqrt{\varepsilon_1} \cos \theta_1 - \sqrt{\varepsilon_2} \cos \theta_2 - \tilde{\sigma}}{\sqrt{\varepsilon_1} \cos \theta_1 + \sqrt{\varepsilon_2} \cos \theta_2 + \tilde{\sigma}} \right|^2, \quad (24)$$

$$R_p = \left| \frac{\sqrt{\varepsilon_2}/\cos \theta_2 - \sqrt{\varepsilon_1}/\cos \theta_1 + \tilde{\sigma}}{\sqrt{\varepsilon_2}/\cos \theta_2 + \sqrt{\varepsilon_1}/\cos \theta_1 + \tilde{\sigma}} \right|^2, \quad (25)$$

$$T_s = \frac{4\sqrt{\varepsilon_1\varepsilon_2} \cos \theta_1 \cos \theta_2}{|\sqrt{\varepsilon_1} \cos \theta_1 + \sqrt{\varepsilon_2} \cos \theta_2 + \tilde{\sigma}|^2}, \quad (26)$$

$$T_p = \frac{4\sqrt{\varepsilon_1\varepsilon_2}/(\cos \theta_1 \cos \theta_2)}{|\sqrt{\varepsilon_2}/\cos \theta_2 + \sqrt{\varepsilon_1}/\cos \theta_1 + \tilde{\sigma}|^2}, \quad (27)$$

where θ_1 and θ_2 are incident and refracted angles, respectively and $\tilde{\sigma} = \sigma/\varepsilon_0 c$. By neglecting the higher-order terms of $\tilde{\sigma}$, the absorbance is given by

$$A_s = \frac{4\sqrt{\varepsilon_1} \cos \theta_1 \text{Re}(\tilde{\sigma})}{(\sqrt{\varepsilon_1} \cos \theta_1 + \sqrt{\varepsilon_2} \cos \theta_2 + \tilde{\sigma})^2}, \quad (28)$$

$$A_p = \frac{4\sqrt{\varepsilon_1} \text{Re}(\tilde{\sigma})/\cos \theta_1}{(\sqrt{\varepsilon_2}/\cos \theta_2 + \sqrt{\varepsilon_1}/\cos \theta_1 + \tilde{\sigma})^2}. \quad (29)$$

Obviously, for a single free-standing graphene layer under normal incidence its absorbance for $\Omega > 2$ is given by $\pi\alpha/(1 + \pi\alpha/2)^2 \sim \pi\alpha$.

In figure 2, the reflectance, transmittance and absorbance at different incident angles for single graphene are shown. Light is incident from the dielectric of ε_1 . Reflection and transmission are altered somewhat with re-

spect to the case without the graphene layer. For $\varepsilon_1 \leq \varepsilon_2$, the absorbance decreases monotonically with increasing incident angle for p polarization, while for s polarization it increases up to a maximum and then decreases monotonically. For $\varepsilon_1 = \varepsilon_2$, the absorbance for s polarization takes a universal value at normal incidence, about $\pi\alpha$ and the maximal absorbance is 0.5 at an incident angle very close to $\pi/2$.

For $\varepsilon_1 > \varepsilon_2$, total internal reflection is expected. With the presence of the graphene layer, there is nearly no change in the critical angle. However, above the critical angle reflectance is no longer *total* (smaller than one). For s polarization, the absorbance around the critical angle is several times larger than the universal value of $\pi\alpha$. This implies that the configuration of total internal reflection could be exploited in measurements of optical conductivity of graphene since it can suppress the signal-to-noise ratio considerably.

B. Double-layer graphene

Consider two graphene layers which are separated by a dielectric of ε_2 with a thickness of d . The dielectric constant of the leftmost dielectric is ε_1 and that of the rightmost dielectric is ε_3 . The transfer matrix of the structure can be obtained from equation (16) as

$$\mathcal{M} = D_{1 \rightarrow 2} P(d) D_{2 \rightarrow 3}, \quad (30)$$

whose elements are given by

$$M_{\mu\nu,m} = \frac{\cos k_{2z}d}{2} A_{\mu\nu,m} + \frac{i \sin k_{2z}d}{2} B_{\mu\nu,m}, \quad (31)$$

where $\mu = 1, 2$ and $\nu = 1, 2$. The parameters $A_{\mu\nu,m}$ and $B_{\mu\nu,m}$ are given by

$$A_{\mu\nu,m} = 1 + (-1)^{\mu+\nu} \eta_m \eta'_m - (-1)^\nu (\xi'_m + \zeta_m \xi_m \eta'_m), \quad (32)$$

$$B_{\mu\nu,m} = (-1)^\mu \eta_m + (-1)^\nu (\eta'_m + \zeta_m \xi_m \eta'_m) - (-1)^{\mu+\nu} \eta_m \xi'_m - \zeta_m \xi_m, \quad (33)$$

where

$$\begin{aligned} \eta_s &= k_{2z}/k_{1z}, & \eta_p &= \varepsilon_1 k_{2z}/\varepsilon_2 k_{1z}, \\ \xi_s &= \sigma \mu_0 \omega / k_{1z}, & \xi_p &= \sigma k_{2z} / \varepsilon_0 \varepsilon_2 \omega, \\ \eta'_s &= k_{3z}/k_{2z}, & \eta'_p &= \varepsilon_2 k_{3z} / \varepsilon_3 k_{2z}, \\ \xi'_s &= \sigma \mu_0 \omega / k_{2z}, & \xi'_p &= \sigma k_{3z} / \varepsilon_0 \varepsilon_3 \omega. \end{aligned} \quad (34)$$

In figure 3, the reflectance, transmittance and absorbance of double-layer graphene for $\varepsilon_1 = \varepsilon_3 = 1$ and $\varepsilon_2 = 2.25$ are shown. For small d , despite different values, the dependence of the reflectance, transmittance and absorbance on the incident angle is, in general, similar to that of single-layer graphene. At normal incidence, the absorbance is nearly twice the universal value of $\pi\alpha$. For large d , however, there are oscillations in reflectance, transmittance and absorbance, which originate from the thin-film interference.

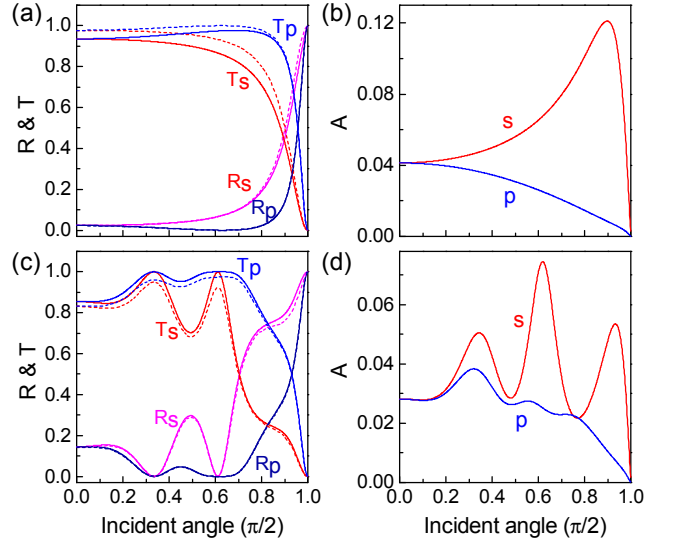


FIG. 3. Reflectance, transmittance and absorbance of double-layer graphene as a function of the incident angle for $\Omega > 2$. Two graphene layers have the same optical conductivity. (a) Reflectance and transmittance for s and p polarizations with $d = 0.1\hbar c/\mu$ (corresponding to $0.132 \mu\text{m}$ for a typical chemical potential $\mu = 0.15 \text{ eV}$). Dashed lines represent those in the absence of the graphene layers. The corresponding absorbance is given in (b). (c) Same as (a) but for $d = 8\hbar c/\mu$ (corresponding to $10.5 \mu\text{m}$ for $\mu = 0.15 \text{ eV}$). The corresponding absorbance is given in (d).

C. Multi-layer graphene

For multi-layer graphene, the transfer matrix can be obtained from equation (16). Reflectance, transmittance and absorbance can be then obtained from equations (19), (20) and (22) respectively.

In figure 4, the reflectance and absorbance of multi-layer graphene at normal incidence are shown. The structure consists of identical graphene layers in air, separated equally by a distance d . At low frequencies the reflectance is close to one up to a certain cutoff frequency. Above the cutoff frequency, for small d the reflectance oscillates and drops rapidly to zero. For large d , however, there appear sharp reflection peaks for frequency above the cutoff frequency, resulting from the multiple interference by the graphene layers.

The structure has zero absorbance for $\Omega < 2$ and shows remarkable absorption for $\Omega > 2$. For small d , the absorbance is nearly a constant, being 0.5 for $\Omega > 2$. With increasing d , multiple interference by graphene layers may play an important role, leading to sharp absorption dips. These interesting properties imply that multi-layer graphene has the potential as dark materials for achieving lower reflection coatings and enhanced photodetection [39].

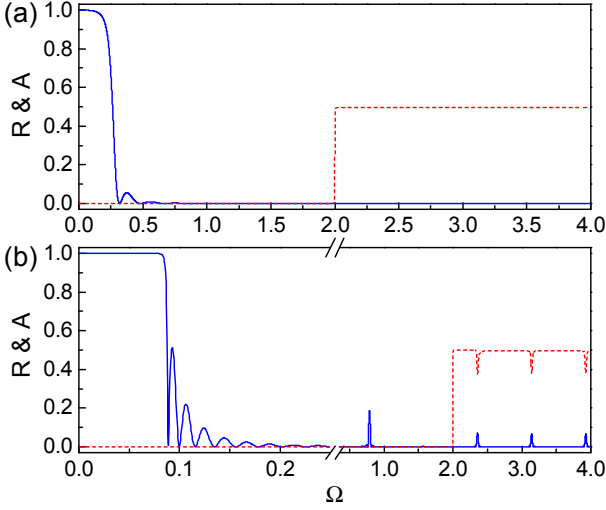


FIG. 4. Reflectance (solid line) and absorbance (dashed line) spectra of multi-layer graphene at normal incidence. There are totally 30 identical graphene layers. (a) $d = 0.1\hbar c/\mu$ and (b) $d = 4\hbar c/\mu$ (corresponding to 0.132 and 5.26 μm for $\mu = 0.15\text{ eV}$, respectively).

IV. PHOTONIC BAND STRUCTURE OF PERIODICAL GRAPHENE LAYERS

When dielectrics are arranged in a periodical way to form so-called photonic crystals [40–42], electromagnetic waves should be strongly modulated by Bragg scatterings, showing photonic band structures with well-defined photonic bands and even photonic bandgaps. For graphene layers stacking in a periodical way, photonic band structures should also be expected due to the introduced periodical modulations.

The first structure considered is shown schematically in figure 5(a). It is composed of identical graphene layers embedded into the interfaces of a one-dimensional photonic crystal consisting of two dielectrics of ε_1 and ε_2 with a thickness of d_1 and d_2 , respectively. For such a structure, its transfer matrix after propagating over one unit cell reads

$$\mathcal{M}_m = D_{1 \rightarrow 2, m} P(d_2) D_{2 \rightarrow 1, m} P(d_1). \quad (35)$$

The photonic band structure can be then obtained from the diagonal elements of the transfer matrix [34], $\cos(qd) = (M_{11, m} + M_{22, m})/2$, where q is the Bloch wave-vector and $d = d_1 + d_2$ is the lattice constant. It can be explicitly written as

$$\begin{aligned} \cos(qd) = & \cos(k_{1z}d_1) \cos(k_{2z}d_2) - \frac{1}{2}(\eta_m + \eta_m^{-1}) \\ & \times \sin(k_{1z}d_1) \sin(k_{2z}d_2) - \Delta_m, \end{aligned} \quad (36)$$

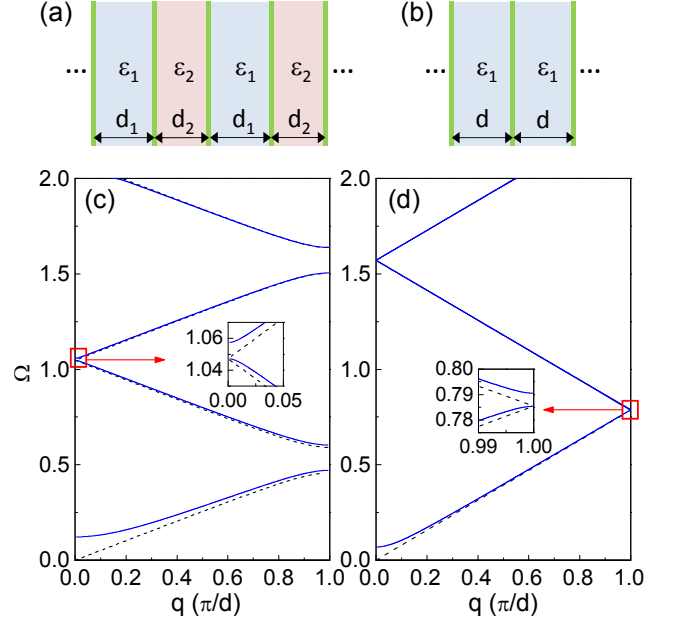


FIG. 5. (a) Schematic of a structure consisting of identical graphene layers placed at the interfaces of a one-dimensional photonic crystal. (b) Schematic of a structure consisting of identical graphene layers separated equally in air. (c) Photonic band structure (solid lines) for the structure in (a). The parameters are $\varepsilon_1 = 1$, $\varepsilon_2 = 2.25$, $d_1 = 3\hbar c/\mu$ and $d_2 = 2\hbar c/\mu$ (corresponding to 2.63 and 3.95 μm for $\mu = 0.1\text{ eV}$, respectively). Dashed lines are the results in the absence of graphene layers. (d) Same as (c) but for the structure in (b). The parameters are $\varepsilon = 1$ and $d = 4\hbar c/\mu$. Dashed lines are simply the folded dispersion in air $\omega = qc$.

where

$$\begin{aligned} \Delta_m = & i\xi_m[(1 + \eta_m^{-1}) \sin(k_{1z}d_1 + k_{2z}d_2) \\ & + \varsigma_m(1 - \eta_m^{-1}) \sin(k_{1z}d_1 - k_{2z}d_2)] \\ & + \frac{\xi_m^2}{2\eta_m} \sin(k_{1z}d_1) \sin(k_{2z}d_2). \end{aligned} \quad (37)$$

Without the term Δ_m , equation (36) reduces to the photonic band structure of a one-dimensional photonic crystal [34].

For identical graphene layers separated equally by a distance d in air as shown in figure 5(b), the transfer matrix simply reads $\mathcal{M}_m = D_m P(d)$, where

$$D_m = \begin{bmatrix} 1 + \xi_m/2 & -\varsigma_m \xi_m/2 \\ \varsigma_m \xi_m/2 & 1 - \xi_m/2 \end{bmatrix}. \quad (38)$$

The photonic band structure of the structure is then given by

$$\cos(qd) = \cos(k_z d) - \frac{i\xi_m}{2} \sin(k_z d), \quad (39)$$

which is identical to that given in reference [43].

In figure 5, the photonic band structures of periodical graphene layers are shown for the propagation direction perpendicular to the graphene layers. For both

structures the first photonic band starts from a certain nonzero cutoff frequency, different from conventional dielectric photonic crystals. This cutoff frequency corresponds exactly to that observed in the reflection spectra shown in figure 4. Below the cutoff frequency, high reflection or low transmission is expected, which was also observed in numerical simulations of a stack of graphene layers separated by dielectric slabs [44]. It is known that in the low-frequency limit periodical metallic structures can be considered as bulk metals with a depressed effective plasma frequency [45, 46]. Thus, periodical graphene layers can also be regarded as a bulk metal with an extremely low effective plasma frequency.

For the structure shown in figure 5(a), the photonic crystal in the absence of graphene layers displays well-defined photonic bands and bandgaps. With the introduction of graphene layers, however, both photonic bands and bandgaps are modified. For example, for the photonic crystal in the absence of graphene layers, there should be no bandgap between the second and third photonic bands since this photonic crystal is a quarter-wave stack. In the presence of graphene layers, however, a mini photonic bandgap opens up.

For the second structure shown in figure 5(b), there should be no photonic bandgaps in the absence of graphene layers. In the presence of graphene layers, however, a series of mini photonic bandgaps appear owing to the multiple interference by graphene layers. It is known that for frequency within photonic bandgaps light propagation is forbidden [40–42]. For a structure consisting of finite graphene layers, this will cause strong reflection for frequency located into the mini photonic bandgaps, as can be clearly seen from figure 4(b).

V. PLASMONS

A flat metal surface can support surface plasmons [24–26] which are transverse magnetic (TM) electromagnetic waves coupled with collective oscillations of surface charges. Surface plasmons can propagate along the metal surface with the fields decaying exponentially away from the both sides of the surface. In doped or gated graphene, free carriers can also support plasmons [17–22]. Owing to the two-dimensional nature and unique electronic band structure, graphene can support not only TM but also transverse electric (TE) plasmons [19]. The later does not exist in conventional metal surfaces.

For a graphene layer surrounded by two dielectrics as shown in figure 1(a), the transfer matrix is simply the transmission matrix. From equation (17), the reflection coefficient of the system can be obtained. The condition for the existence of plasmons is that the reflection coefficient has poles, namely

$$1 + \eta_m + \zeta_m \xi_m = 0, \quad (40)$$

where the subscript m stands for s and p polarization, corresponding to TE and TM modes, respectively.

From equation (40), the dispersion of TM plasmons can be obtained as

$$\frac{\varepsilon_1}{\sqrt{Q^2 - \varepsilon_1 \Omega^2}} + \frac{\varepsilon_2}{\sqrt{Q^2 - \varepsilon_2 \Omega^2}} = -\frac{i\sigma(\Omega)/\varepsilon_0 c}{\Omega}, \quad (41)$$

with $Q \equiv \hbar c q / \mu$, where $q (\equiv k_x)$ is the wave-vector of the plasmons. Obviously, TM plasmons can exist if the imaginary part of σ is *positive*. From the above equation, TM plasmons are far below the light line, i.e., $q \gg \omega/c$. Thus, in this non-retarded regime, the dispersion of TM plasmons is simplified to

$$Q = -(\varepsilon_1 + \varepsilon_2) \Omega (\varepsilon_0 c) / i\sigma. \quad (42)$$

For $\Omega > 2$, σ has a real value as well, leading to a strong loss due to interband excitations. For small q , the dispersion of TM plasmons reduces to

$$\Omega = 2 \sqrt{\frac{\alpha}{(\varepsilon_1 + \varepsilon_2)}} Q, \quad (43)$$

which shows the known \sqrt{q} -dependence [17, 18].

From equation (40), the dispersion of TE plasmons is given by

$$\sqrt{Q^2 - \varepsilon_1 \Omega^2} + \sqrt{Q^2 - \varepsilon_2 \Omega^2} = \frac{i\sigma}{\varepsilon_0 c} \Omega, \quad (44)$$

which is the same as that given in reference [19]. TE plasmons can exist if $\varepsilon_1 = \varepsilon_2$ and the imaginary part of σ is *negative* (for $\Omega > 1.667$). Note that the term on the right side of the above equation is very small in the frequency window $1.667 < \Omega < 2$. As a result, the dispersion of TE plasmons should be below but very close to the light line $\omega = qc/\sqrt{\varepsilon_1}$.

We now consider a structure where a graphene layer is apart from a dielectric substrate of ε_2 over a distance of d , as shown schematically in the inset of figure 6. For the structure, TE plasmons do not exist for finite d and thus we only discuss TM plasmons. For p polarization, the transfer matrix of the structure can be obtained from equation (16), namely

$$\mathcal{M} = DP(d)D', \quad (45)$$

where

$$D = \frac{1}{2} \begin{bmatrix} 1 + \eta_p + \xi_p & 1 - \eta_p - \xi_p \\ 1 - \eta_p + \xi_p & 1 + \eta_p - \xi_p \end{bmatrix}, \quad (46)$$

$$D' = \frac{1}{2} \begin{bmatrix} 1 + \eta'_p & 1 - \eta'_p \\ 1 - \eta'_p & 1 + \eta'_p \end{bmatrix}, \quad (47)$$

$$P = \begin{bmatrix} e^{-ik_{1z}d} & 0 \\ 0 & e^{ik_{1z}d} \end{bmatrix}, \quad (48)$$

with

$$\eta_p = 1, \quad \xi_p = \sigma k_{1z} / \varepsilon_0 \varepsilon_1 \omega, \quad \eta'_p = \varepsilon_1 k_{2z} / \varepsilon_2 k_{1z}. \quad (49)$$

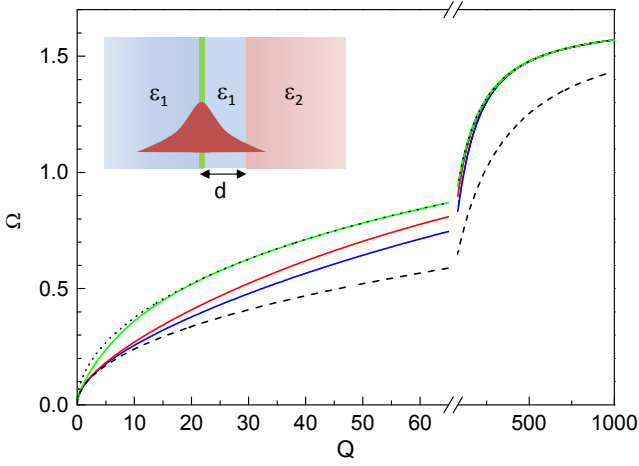


FIG. 6. Dispersion of TM plasmons for a structure shown in the inset where the graphene layer is apart from a dielectric substrate of $\varepsilon_2 = 10$ over a distance of d and the other dielectrics are air with $\varepsilon_1 = 1$. Blue, green and red lines are the results for $\tilde{d} = 0.005, 0.01$ and 0.1 , respectively. The dotted line represents the dispersion for a free-standing graphene layer in air and the dashed line corresponds to the case $d = 0$.

With the transfer matrix, it is easy to obtain the reflection coefficient from equation (17). The condition for the existence of plasmons thus reads

$$(1 + \eta_p + \xi_p)(1 + \eta'_p) e^{-ik_{1z}d} + (1 - \eta_p - \xi_p)(1 - \eta'_p) e^{ik_{1z}d} = 0. \quad (50)$$

Since the dispersion of graphene plasmons lies far below the light line, the non-retarded condition $q \gg \omega/c$ still holds, leading to $\eta'_p \simeq \varepsilon_1/\varepsilon_2$ and $\xi_p \simeq i\sigma q/\varepsilon_0\varepsilon_1\omega$. Thus, plasmon dispersion can be simplified as

$$\frac{2\varepsilon_1(\varepsilon_1 + \varepsilon_2)}{(\varepsilon_1 + \varepsilon_2) + (\varepsilon_1 - \varepsilon_2)e^{-2Q\tilde{d}}} = -\frac{i\sigma}{\varepsilon_0c} \frac{Q}{\Omega}, \quad (51)$$

where $\tilde{d} = d\mu/\hbar c$.

In figure 6, the dispersion of TM plasmons for the structure shown in the inset is given. The separation of the graphene layer from the dielectric substrate of ε_2 affects considerably the dispersion. For small q , the dispersion takes that for the case of $d = 0$. For large q , it approaches that for the free-standing case. This dispersion interchange with increasing q can be understood by the fact that the fields of plasmons decay exponentially into the surrounding media, as schematically depicted in the inset. For small q , the decay length is much larger than d such that the fields concentrate dominantly in the substrate. As a result, the dispersion should take that for the case $d \sim 0$. For large q , the fields decay very fast such that the decay length is much smaller than d . In this situation, the fields could not sense the substrate dielectric layer.

Obviously, the dispersion interchange can be tuned by d . The change from one kind of dispersion to the other

occurs faster for large d than for small d . Practically, we may adopt this dispersion interchange to tune the dispersion of TM plasmons, or in other words, the refractive index of the plasmons. From equation (42), the corresponding refractive index of TM plasmons for a graphene layer surrounded by two dielectrics of ε_1 and ε_2 is given by

$$n_p \equiv qc/\omega = -\frac{\varepsilon_1 + \varepsilon_2}{i\sigma/\varepsilon_0c}. \quad (52)$$

With the structure shown in the inset of figure 6, the refractive index of TM plasmons can thus be tuned from $-2\varepsilon_1/(i\sigma/\varepsilon_0c)$ to $-(\varepsilon_1 + \varepsilon_2)/(i\sigma/\varepsilon_0c)$. This offers practically a simple approach to manipulate the dispersion of TM plasmon or the refractive index by changing d .

VI. CONCLUSIONS

In the present paper, we developed a transfer matrix method for optical calculations in non-interacting graphene layers. With the framework of this method, the transfer matrix for various graphene layers can be obtained. With the transfer matrix, reflectance, transmittance and absorbance spectra of graphene layers can be easily obtained. In addition, photonic band structures for periodical graphene layers and even graphene plasmons can be studied in a rather simple way.

Using the transfer matrix method, we studied the optical properties such as reflection, transmission and absorption for single-, double- and multi-layer graphene. We showed that the configuration of total internal reflection in single-layer graphene and thin-film interference effects in double-layer graphene could be exploited to enhance the light absorption. For multi-layer graphene, there exists a cutoff frequency below which the reflectance is as high as one. For a small spacing distance, the absorbance is as high as 50% for $\Omega > 2$. With increasing spacing distance, sharp reflection peaks and absorption dips appear owing to the multiple interference by graphene layers.

We applied the transfer matrix method to structures consisting of periodically arranged identical graphene layers. The structures are characterized by photonic band structures with well-defined photonic bands and bandgaps. We revealed that these structures can be regarded as bulk metals with an extremely low effective plasma frequency.

Finally, we discussed plasmons in a graphene layer which is apart from a dielectric substrate. We found that the plasmon dispersion can be tuned by the separating distance between the graphene layer and the dielectric substrate. Our results show that the transfer matrix method could serve as a versatile tool to study optical properties in graphene layers.

VII. ACKNOWLEDGMENT

This work was supported by the 973 Program (Grant Nos. 2013CB632701 and 2011CB922004). The research of J.Z. and X.H.L. is further supported by the NSFC.

-
- [1] Novoselov K S, Geim A K, Morozov S V, Jiang D, Zhang Y, Dubonos S V, Grigorieva I V and Firsov A A 2004 *Science* **306** 666
 - [2] Wilson M 2006 *Phys. Today* **59** 21
 - [3] Castro Neto A H, Guinea F, Peres N M R, Novoselov K S and Geim A K 2009 *Rev. Mod. Phys.* **81** 109
 - [4] Nair R R, Blake P, Grigorenko A N, Novoselov K S, Booth T J, Stauber T, Peres N M R and Geim A K 2008 *Science* **320** 1308
 - [5] Kuzmenko A B, van Heumen E, Carbone F, and van der Marel D 2008 *Phys. Rev. Lett.* **100**, 117401
 - [6] Stauber T, Peres N M R and Geim A K 2008 *Phys. Rev. B* **78** 085432
 - [7] Mak K F, Sfeir M Y, Wu Y, Lui C H, Misewich J A and Heinz T F 2008 *Phys. Rev. Lett.* **101** 196405
 - [8] Wang F, Zhang Y, Tian C, Girit C, Zettl A, Crommie M and Shen Y R 2008 *Science* **320** 206
 - [9] Li Z Q, Henriksen E A, Jiang Z, Hao Z, Martin M C, Kim P, Stormer H L and Basov D N 2008 *Nat. Phys.* **4** 532
 - [10] Casiraghi C, Hartschuh A, Lidorikis E, Qian H, Harutyunyan H, Gokus T, Novoselov K S and Ferrari A C 2007 *Nano Lett.* **7** 2711
 - [11] Bae S, Kim H, Lee Y, Xu X, Park J S, Zheng Y, Balakrishnan J, Lei T, Ri Kim H, Song Y I, Kim Y J, Kim K S, Ozyilmaz B, Ahn J H, Hong B H and Iijima S 2010 *Nat. Nano.* **5** 574
 - [12] Jo G, Choe M, Cho C Y, Kim J H, Park W J, Lee S, Hong W K, Kim T W, J. P S, Hong B H, Kahng Y H and Lee T 2010 *Nanotechnology* **21** 175201
 - [13] Xia F, Mueller T, Lin Y, Valdes-Garcia A and Avouris P 2009 *Nat. Nano.* **4** 839
 - [14] Stauber T and Gmez-Santos G 2012 *Phys. Rev. B* **85** 075410
 - [15] Sun Z, Hasan T, Torrisi F, Popa D, Privitera G, Wang F, Bonaccorso F, Basko D M and Ferrari A C 2010 *ACS. Nano* **4** 803
 - [16] Liu M, Yin X, Ulin-Avila E, Geng B, Zentgraf T, Ju L, Wang F and Zhang X 2011 *Nature* **474** 64
 - [17] Wunsch B, Stauber T, Sols F and Guinea F 2006 *New J. Phys.* **8** 318
 - [18] Hwang E H and Das Sarma S 2007 *Phys. Rev. B* **75** 205418
 - [19] Mikhailov S A and Ziegler K 2007 *Phys. Rev. Lett.* **99** 016803
 - [20] Liu Y, Willis R F, Emtsev K V and Seyller T 2008 *Phys. Rev. B* **78** 201403
 - [21] Jablan M, Buljan H and Soljačić M 2009 *Phys. Rev. B* **80** 245435
 - [22] Profumo R E V, Polini M, Asgari R, Fazio R and MacDonald A H 2010 *Phys. Rev. B* **82** 085443
 - [23] Fei Z, Andreev G O, Bao W, Zhang L M, McLeod A S, Wang C, Stewart M K, Zhao Z, Dominguez G, Thieme M, Fogler M M, Tauber M J, Castro-Neto A H, Lau C N, Keilmann F and Basov D N 2011 *Nano Lett.* **11** 4701
 - [24] Raether H 1998 *Surface Plasmons* (Berlin: Springer-Verlag)
 - [25] Barnes W L, Dereux A and Ebbesen T W 2003 *Nature* **424** 824
 - [26] Maier S A 2007 *Plasmonics: Fundamentals and Applications* (New York: Springer)
 - [27] Ju L, Geng B, Horng J, Girit C, Martin M, Hao Z, Bechtel H A, Liang X, Zettl A, Shen Y R and Wang F 2011 *Nat. Nano.* **6** 630
 - [28] Vakil A and Engheta N 2011 *Science* **332** 1291
 - [29] Nikitin A Y, Guinea F, Garca-Vidal F J and Martn-Moreno L 2011 *Phys. Rev. B* **84** 161407
 - [30] Thongrattanasiri S, Koppens F H L and Garca de Abajo F J 2012 *Phys. Rev. Lett.* **108** 047401
 - [31] Yan H, Li X, Chandra B, Tulevski G, Wu Y, Freitag M, Zhu W, Avouris P and Xia F 2012 *Nat. Nano.* **7** 330
 - [32] Bonaccorso F, Sun Z, Hasan T and Ferrari A C 2010 *Nat. Photon.* **4** 611
 - [33] Yeh P 1988 *Optical Waves in Layered Media* (New York: Wiley)
 - [34] Zi J, Wan J and Zhang C 1998 *Appl. Phys. Lett.* **73** 2084
 - [35] Jackson J D 2001 *Classical Electrodynamics* third edn (New York: Wiley) p 16
 - [36] Ando T, Zheng Y and Suzuura H 2002 *J. Phys. Soc. Jpn.* **71** 1318
 - [37] Gusynin V P, Sharapov S G and Carbotte J P 2006 *Phys. Rev. Lett.* **96** 256802
 - [38] Falkovsky L A and Varlamov A A 2007 *Eur. Phys. J. B* **56** 281
 - [39] Ludwig A and Webb K J 2011 *Opt. Lett.* **36** 106
 - [40] Yablonovitch E 1987 *Phys. Rev. Lett.* **58** 2059
 - [41] John S 1987 *Phys. Rev. Lett.* **58** 2486
 - [42] Joannopoulos J D, Johnson S G, Winn J N and Meade R D 2008 *Photonic Crystals: Molding the Flow of Light* second edn (Princeton, NJ: Princeton University Press)
 - [43] Falkovsky L A and Pershoguba S S 2007 *Phys. Rev. B* **76** 153410.
 - [44] Kaipa C S R, Yakovlev A B, Hanson G W, Padooru Y R, Medina F and Mesa F 2012 *Phys. Rev. B* **85** 245407
 - [45] Pendry J B, Holden A J, Stewart W J and Youngs I 1996 *Phys. Rev. Lett.* **76** 4773
 - [46] Xu X, Xi Y, Han D, Liu X, Zi J and Zhu Z 2005 *Appl. Phys. Lett.* **86** 091112